AJNR Am J Neuroradiol 19:1055–1060, June 1998

Comparison of T2 Lesion Volume and Magnetization Transfer Ratio Histogram Analysis and of Atrophy and Measures of Lesion Burden in Patients with Multiple Sclerosis

Micheal D. Phillips, Robert I. Grossman, Yukio Miki, Lougang Wei, Dennis L. Kolson, Mark A. van Buchem, Marcy Polansky, Joseph C. McGowan, and Jayaram K. Udupa

PURPOSE: **The purpose of this study was twofold: first, to compare two different measures of lesion burden in patients with multiple sclerosis (MS), the magnetization transfer ratio (MTR) histogram and T2 lesion volume; and, second, to investigate the relationship between lesion burden and atrophy in patients with MS.**

METHODS: **Thirty patients with MS were examined with MR imaging, including fast spin-echo T2- and proton density–weighted sequences as well as magnetization transfer sequences. The lesion burden in each subject was quantitated by MTR histographic analysis and by a computer-based method for calculating the total volume of lesions on T2-weighted images. Additionally, the CSF volume, the brain parenchymal volume, and the percentage of brain parenchymal volume were determined in all patients by using this method and were compared with measurements in eight control subjects.**

RESULTS: **Significant loss of parenchymal volume was seen in patients with MS as determined by increased CSF volume and decreased percentage of brain parenchymal volume relative to that in age-matched control subjects. An inverse correlation was observed between the peak height of the MTR histogram and T2 lesion volume. T2 lesion volume corresponded positively with CSF volume and inversely with percentage of brain parenchymal volume. The peak height of the MTR histogram corresponded positively with percentage of brain parenchymal volume and inversely with CSF volume.**

CONCLUSION: **MS patients sustain a significant loss of parenchymal volume (atrophy), which corresponds strongly with increasing lesion burden. T2 lesion volume and peak height of the MTR histogram show good correlation, and the peak height of the MTR histogram shows a superior correlation with measures of brain atrophy as compared with measurements of T2 lesion volume, suggesting that the MTR histogram may be a better indicator of global disease burden than is T2 lesion volume.**

MR imaging is the most sensitive radiologic method for evaluating multiple sclerosis (MS) (1, 2). Lesions identified on conventional T1-, T2-, and proton density–weighted images have been shown to correspond with macroscopically observed MS plaques on pathologic analysis (3, 4). Lesion burden, as based on conventional MR imaging findings, has been quantitated by a variety of methods (5–9), including a computerized technique that has an inter- and intraobserver variability of less than 1% (10). Although it is possible to characterize the volume of macroscopic lesions, it is unlikely that this measurement reflects the full extent of lesion burden in patients with MS. One study involving 14 patients with MS demonstrated that on pathologic evaluation, up to 72% of the samples of macroscopically normal-appearing white matter had microscopic abnormalities (11). Microscopic changes included diffuse gliosis,

Received September 29, 1997; accepted after revision January 25, 1998.

Supported in part by RSNA Research and Education Fund Fellowship Award and by grants NS29029, NS34353, and M01-RR00044 from the National Institutes of Health.

From the Departments of Radiology (M.D.P., R.I.G., Y.M., L.W., J.C.M., J.K.U.) and Neurology (D.L.K.), Hospital of the University of Pennsylvania, Philadelphia, PA; the Department of Radiology, Leiden University Hospital, Leiden, the Netherlands (M.A.v.B.); and the Division of Biometrics, Hahnemann University, Philadelphia, PA (M.P.).

Address reprint requests to Robert I. Grossman, MD, Department of Radiology, Neuroradiology Section, Hospital of the University of Pennsylvania, 3400 Spruce St, Philadelphia, PA 19104.

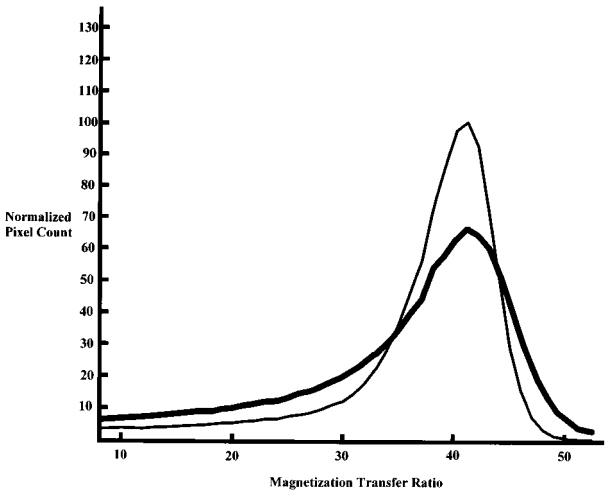

FIG 1. MTR histograms in a control subject (*thin line*) and a patient with MS (*thick line*). MTR values are displayed along the *x*-axis and normalized pixel counts are displayed along the *y*-axis. The peak height of the histogram (the MTR value with the largest normalized pixel count) is decreased in the MS patient as compared with that of the control subject.

perivascular infiltration, and small foci of demyelination (11). Consistent with these results, areas of normal-appearing white matter on standard fast spin-echo (FSE) MR images in patients with MS have been shown to be abnormal when examined with magnetization transfer imaging, spectroscopy, or calculated relaxation times (12–17). Dousett et al (12) noted that individual lesions observed on FSE T2-weighted MR images displayed markedly decreased magnetization transfer ratio (MTR) values and that the MTR was also decreased, although to a lesser extent, in normal-appearing white matter. Several studies have subsequently confirmed that the MTR is significantly reduced in areas of normal-appearing white matter in patients with MS (13–15). The abnormal MTRs in normal-appearing white matter have been attributed to the microscopic changes seen at pathologic examination (13).

Van Buchem et al (18) reported a highly automated, objective method for evaluating changes in the MTR throughout the entire brain. With this technique, the extracranial contents are excluded and then a voxel-by-voxel calculation of the MTR is performed on the intracranial contents. This method was used to compute whole-brain histograms (see Fig 1). Van Buchem et al showed that the peak height of these MTR histograms is decreased in patients with MS as compared with that in subjects without disease. On the basis of these results, the MTR histogram has been suggested as a good indicator of whole-brain disease burden in patients with MS, because it reflects the macroscopic lesions detected on both conventional MR and magnetization transfer images as well as the microscopic lesions seen only with magnetization transfer imaging (18).

The relationship, if any, between the MTR histogram and the volume of MS lesions seen on standard FSE T2-weighted MR images has not been addressed. The present study was designed to investigate this relationship. Specifically, we compared the normalized peak height of the histogram with the total lesion volume on FSE T2-weighted MR images. Our hypothesis was that these measures of lesion burden should have an inverse relationship. Additionally, we evaluated the relationship between loss of parenchymal volume (atrophy) and lesion burden as measured by both peak height of the MTR histogram and T2 lesion volume. We hypothesized that atrophy would correspond with T2 lesion volume and that there would be an inverse relationship between peak height of the histogram and degree of parenchymal loss.

Methods

The subjects were part of a cohort of patients enrolled in a long-term NIH-funded study to quantitatively evaluate MR lesion burden in persons with MS. There were 21 women and nine men (27 to 58 years old) with clinically definite MS as defined by the Poser criteria (19). Ten patients had chronic-progressive MS (mean duration of disease, 5.7 years at the time of imaging) and the remaining 20 had relapsing-remitting MS (mean duration of disease, 4.6 years at the time of imaging). Subjects were untreated except for brief courses (2 to 3 weeks) of pulsed corticosteriods for exacerbations of symptoms. Two patients had received steroids in the 6 months prior to imaging with treatment stopped at 3 months before imaging in one case and at 3.5 weeks before imaging in the other. The rest of the patients had not received steroids within 6 months of their imaging date. Eight age-matched volunteers with no history of neurologic illness were used as control subjects. All had normal findings on brain MR images as interpreted by an experienced neuroradiologist.

All examinations were performed on the same 1.5-T clinical MR system with a quadrature head coil. The imaging protocol consisted of whole-brain sagittal T1-weighted localizer images (600/17 [TR/TE]) with a section thickness of 5 mm, and axial FSE T2-weighted images (2500/18,90) with a section thickness of 3 mm. Magnetization transfer imaging was performed with a standard 3-D sequence (106/5) with gradient-recalled acquisition in the steady state and a flip angle of 12°. Images were obtained at 5-mm intervals both with and without a saturation pulse applied. The saturation pulse consisted of a 19-millisecond single-cycle sync pulse with an average radio frequency field intensity of 3.67×10^{-6}T, which was applied at a frequency of 2 kHz below water resonance. The interval between the end of the saturation pulse and the beginning of each excitation was approximately 1 millisecond. This pulse sequence was chosen to minimize T1 and T2 effects.

The volume of MS lesions was calculated by using a validated semiautomated computerized method with a known inter- and intraobserver variability of less than 1% (10). The method is based on the concept of fuzzy connectivity (22) and is incorporated in a software system called 3DVIEWNIX (21) that has been described previously (22, 23). The volume measurements were performed by the same neuroradiologist in all cases.

The calculations for parenchymal and CSF volumes were also performed using the 3DVIEWNIX system. The calculation involves the production of a CSF-only image (see Fig 2) from which the measurement of the CSF volume is made. The process begins with segmentation of the extracranial contents, which can be done after briefly training the program by having the observer identify white matter, gray matter, and CSF using a previously described method (22, 23). All the segmented sections were then reviewed and any residual extracranial components excluded, if need be, by an operator. An angle image

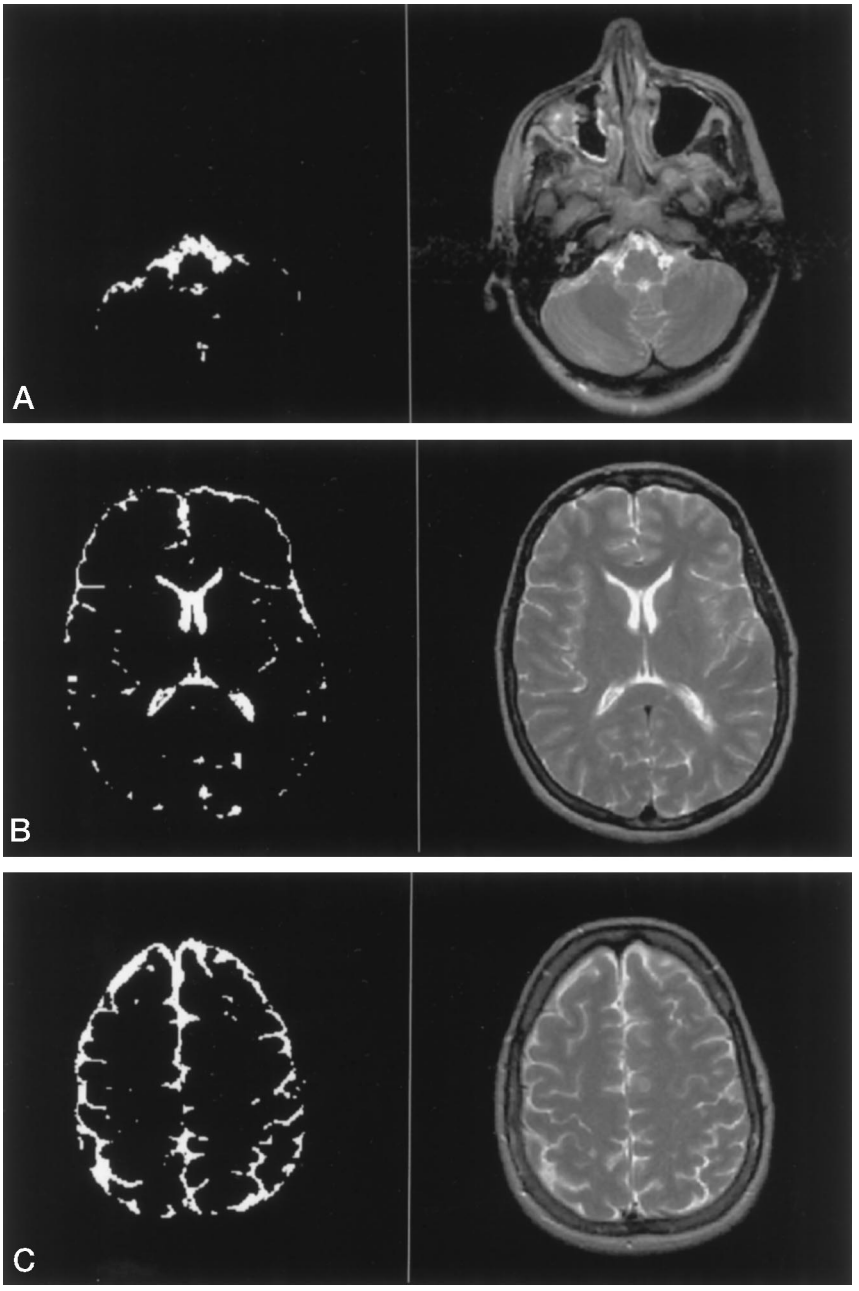

FIG 2. *A–C*, CSF-only images (*left*) and corresponding FSE T2-weighted (2500/90/1) images (*right*) at the level of the posterior fossa (*A*), lateral ventricles (*B*), and cerebral convexities (*C*).

was then produced from the segmented T2- and proton density–weighted data sets using the method described by Udupa et al (20). In brief, this technique creates a voxel-by-voxel image using the following formula $I_{angle} = \tan{-}1\ (I_{T2}/I_{PD})$, where I_{angle}, I_{T2}, and I_{PD} are the intensities of the voxels from the angle and from the T2- and proton density–weighted images, respectively. The power of the angle image comes from its effective elimination of the wide variation in CSF intensities commonly seen on T2- and proton density–weighted images due to inhomogeneity in the magnetic field. The resulting angle image has relatively homogeneous CSF intensity values. A threshold intensity value was then applied to the angle image to produce a CSF-only image. The threshold value was selected by using the T2-weighted images as a guide to produce a CSF-only image, which accurately reflects the CSF volume (see Fig 2). Both the segmentation and thresholding were performed by a single neuroradiologist. The CSF volume was calculated by summing the total volume of the voxels in the CSF-only image. The value for total brain parenchymal volume was calculated by subtracting the CSF volume from the volume of the intracranial contents (brain parenchymal volume + CSF volume) after segmentation. To normalize for baseline differences in brain parenchymal volume among subjects, an additional parameter, the percentage of brain parenchyma, was also calculated. This was done by using the expression

$$\text{Percentage of brain parenchyma} = \text{brain parenchymal volume/volume of intracranial contents} \times 100$$

MTR histographic analysis was performed using the method described by van Buchem et al (18). Magnetization transfer images were segmented to remove the extracranial contents. Then, for each voxel, MTR was computed using the expression

$$\text{MTR} = [(\text{Mo}-\text{Ms})/\text{Mo}] \times 100$$

where Mo and Ms represent the signal intensity of the voxel with saturation pulse off and on, respectively. The CSF was

separated from other intracranial voxels using a threshold of MTR = 5%. A normalized histogram of the MTR values for the 3-D brain parenchymal region was then computed (see Fig 1). Normalization was achieved by dividing each histogram frequency value (ie, the total number of pixels containing a certain MTR value) by the volume of the intracranial contents to account for variation in head size among patients. The peak height of the histogram is simply the largest normalized frequency (ie, the largest normalized pixel value among the spectrum of individual MTRs). The histographic analysis was performed in all cases by one neuroradiologist.

Statistics were computed with SAS software (SAS Institute, Cary, NC). The data on T2 lesion volume, peak height of the histogram, CSF volume, brain parenchymal volume, and percentage of brain parenchymal volume were analyzed using Spearman correlations. MS patients and control subjects were compared by using the Wilcoxon rank sum test.

Results

The CSF volume was significantly larger in patients with MS than in the age-matched control subjects ($P = .0049$). Additionally, the percentage of brain parenchyma was significantly smaller in MS patients than in the control subjects ($P = .0045$). No significant difference in brain parenchymal volume was seen between the patients and the control subjects ($P = .349$).

A positive correlation was found between T2 lesion volume and CSF volume, with a Spearman correlation coefficient of .730 ($P = .0001$). No correlation was seen between T2 lesion volume and brain parenchymal volume. There was, however, a significant inverse correlation between T2 lesion volume and percentage of brain parenchymal volume, with a Spearman correlation coefficient of $-.746$ ($P = .0001$).

An inverse correlation was found between the peak height of the histogram and the T2 lesion volume, with a Spearman correlation coefficient of $-.728$ ($P = .0001$).

A positive correlation was seen between the peak histogram height and the percentage of brain parenchymal volume, with a Spearman correlation coefficient of .832 ($P = .0001$). An inverse correlation was seen between peak histogram height and CSF volume, with a Spearman correlation coefficient of $-.828$ ($P = .0001$). No correlation was seen between peak height of the histogram and brain parenchymal volume.

Discussion

Generalized atrophy and ventricular enlargement in patients with MS were first described in the pathology literature (24–27). CT studies showed atrophy in patients with long-standing MS (28–31); however, the majority of these studies relied on a subjective assessment of atrophy. Quantitative measurements were performed in several studies (32–35), including one in which an automated computerized technique was used (36). However, CT is less sensitive than MR imaging in depicting the full extent of white matter lesions, so the precise relationship between lesion volume and atrophy remained uncertain.

MR imaging can depict the presence of atrophy of the corpus callosum as well as generalized parenchymal atrophy in patients with MS (37–43). These studies also relied on predominately subjective measurements of atrophy and/or the volume of MS lesions seen on T2-weighted images. One group of investigators (44) did perform objective measurements of lesion volume and parenchymal volume in a study that evaluated the relationship between T2 lesion volume and the change in parenchymal volume on four contiguous brain sections over an 18-month period. There are few data, however, comparing the extent of lesion burden seen on T2-weighted images and the degree of whole-brain parenchymal atrophy, nor are there any studies that have examined the relationship between generalized atrophy and MTR values in patients with MS.

The data from the present study reveal a relationship between lesion volume seen on FSE T2-weighted MR images and reduction in peak height of MTR histograms. This correlation is expected, because individual MS lesions seen on FSE T2-weighted MR images have been shown to have decreased MTRs (12, 15, 45). Hence, an increasing volume of lesions increases the number of voxels with lower MTRs, thereby contributing to a decrease in the peak height of the MTR histogram. Although this result is expected, the association between this MTR histographic parameter and T2 lesion volume has important connotations. If MTR histograms are to be used as a surrogate and potentially more sensitive monitor of lesion burden, they must first be shown to correspond to conventional measures of lesion volume. MTR histograms correspond well to global disease burden seen on FSE T2-weighted images and may additionally depict lesions that are not seen on FSE MR images.

Our data indicate that global volume loss is manifested by an increase in CSF volume and a decrease in percentage of brain parenchymal volume in patients with MS as compared with age-matched healthy volunteers. No significant difference was seen between the patients and the control subjects in the volume of brain parenchyma. Additionally, no correlation was seen between measures of lesion burden and brain parenchymal volume, which most likely reflects variations in brain volume among individuals. Changes in parenchymal volume may be relatively small as compared with differences in parenchymal volume among individuals. The percentage of brain parenchyma normalizes for differences in brain parenchymal volume among subjects, and the sample size of the present study is most likely too small to detect changes in parenchymal volume without normalizing for these individual differences. The total volume of CSF is smaller than that of brain parenchyma and may demonstrate less variation among individuals. Additionally, the CSF volume is relatively smaller than brain parenchymal volume, and may therefore be more sensitive to smaller degrees of loss of parenchymal volume.

Our study shows a correlation between measures of lesion burden and volume loss. Losseff et al (44) found no correlation between baseline or change in T2 lesion burden and the development of atrophy over an 18-month period. This apparent discrepancy between our findings and theirs most likely stems from several differences between the two studies. First, we compared lesion burden with volume loss at single points in time rather than over a period of time. Second, our measurements of lesion burden and volume loss were performed on the whole brain rather than on four contiguous sections, as done by Losseff et al. And, finally, Losseff et al looked at brain parenchymal volume, which showed no significant correlation in our study, rather than CSF volume or percentage of brain parenchymal volume.

Although CSF volume and percentage of brain parenchymal volume both showed a strong correlation with T2 lesion volume (positive and negative, respectively), they showed a stronger correlation with peak height of the histogram. Loss of parenchymal volume in MS most likely reflects a combination of pathologic processes, including demyelination, gliosis, and neuronal loss. The net effect of these pathologic processes results in loss of brain parenchyma. FSE T2-weighted MR imaging is sensitive only to the areas of macroscopic disease. There is evidence to suggest that magnetization transfer imaging can detect macroscopic and microscopic disease as well as neuronal loss (12–15, 46). The increased sensitivity of magnetization transfer imaging as compared with FSE T2-weighted imaging results in superior correlation of the peak height of the MTR histogram with global volume loss. This finding supports the hypothesis that the MTR histogram may offer a better quantification of total disease burden in patients with MS than provided by volume measurements on FSE T2-weighted images.

Conclusion

Our findings of a correlation between the peak height of the MTR histogram and T2 lesion volume and of a better correlation between MTR histogram and loss of parenchymal volume suggest that MTR histograms can be used as a reliable, potentially superior method for quantifying total disease burden in patients with MS. Hence, MTR histograms may offer an important surrogate measure of lesion burden in these patients.

References

1. Jackson JA, Leake DR, Schneiders NJ, et al. **Magnetic resonance imaging in multiple sclerosis: results in 32 cases.** *AJNR Am J Neuroradiol* 1985;6:171–176
2. Jacobs L, Kinkel WR, Polachini I, Kinkel RP. **Correlations of nuclear magnetic resonance imaging, computerized tomography, and clinical profiles in multiple sclerosis.** *Neurology* 1986;36:27–34
3. Stewart WA, Hall LD, Berry K, Paty DW. **Correlation between NMR scan and brain slice data in multiple sclerosis.** *Lancet* 1984; 2:412
4. Ormerod IEC, Miller DH, Mcdonald WI, et al. **The role of NMR imaging in the assessment of multiple sclerosis and isolated neurological lesions: a quantitative study.** *Brain* 1987;110:1579–1616
5. Isaac C, Li DK, Genton M, et al. **Multiple sclerosis: a serial study using MRI in relapsing patients.** *Neurology* 1988;38:1511–1515
6. Uhlenbrock D, Herbe E, Seidel D, Gehlen W. **One-year MR imaging follow-up of patients with multiple sclerosis under cortisone therapy.** *Neuroradiology* 1989;31:3–7
7. Miller DH, Barkhof F, Nauta JJ. **Gadolinium enhancement increases the sensitivity of MRI in detecting disease activity in multiple sclerosis.** *Brain* 1993;116:1077–1094
8. Paty DW, Li DK. **Interferon beta-1b is effective in relapsing-remitting multiple sclerosis, II: MRI analysis results of a multicenter, randomized, double-blind, placebo-controlled trial (UBC MS/MRI Study Group and the IFNB Multiple Sclerosis Study Group).** *Neurology* 1993;43:662–667
9. Frank JA, Stone LA, Smith ME, Albert PS, Maloni H, McFarland HF. **Serial contrast-enhanced magnetic resonance imaging in patients with early relapsing-remitting multiple sclerosis: implication for treatment trials.** *Ann Neurol* 1994;36:S86–S90
10. Samarasekera S, Udupa JK, Miki Y, Wei L, Grossman RI. **A new computer assisted method for enhancing lesion quantification in multiple sclerosis.** *J Comput Assist Tomogr* 1997;21:145–151
11. Allen IV, Mckeown SR. **A histological, histochemical and biochemical study of the macroscopically normal white matter in multiple sclerosis.** *J Neurol Sci* 1979;41:81–91
12. Dousset V, Grossman RI, Ramer KN, et al. **Experimental allergic encephalomyelitis and multiple sclerosis: lesion characterization with magnetization transfer imaging.** *Radiology* 1992;182:483–491
13. Loevner LA, Grossman RI, Cohen JA, Lexa FJ, Kessler D, Kolson DL. **Microscopic disease in normal-appearing white matter on conventional MR images in patients with multiple sclerosis: assessment with magnetization-transfer measurements.** *Radiology* 1995;196:511–515
14. Filippi M, Campi A, Dousset V, et al. **A magnetization transfer imaging study of normal-appearing white matter in multiple sclerosis.** *Neurology* 1995;45:478–482
15. Finelli DA, Hurst GC, Amantia P, Gullapali RP, Apicella A. **Cerebral white matter: technical development and clinical applications of effective magnetization transfer (MT) power concepts for high-power, thin-section, quantitative MT examinations.** *Radiology* 1996;199:219–226
16. Hiehle JFJ, Lenkinski RE, Grossman RI, et al. **Correlation of spectroscopy and magnetization transfer imaging in the evaluation of demyelinating lesions and normal appearing white matter in multiple sclerosis.** *Magn Reson Med* 1994;32:285–293
17. Barbosa S, Blumhardt LD, Roberts N, Lock T, Edwards RH. **Magnetic resonance relaxation time mapping in multiple sclerosis: normal appearing white matter and the invisible lesion load.** *Magn Reson Imaging* 1994;12:33–42
18. Van Buchem MA, Udupa JK, Heyning FH, et al. **Volumetric quantitation of intracranial macroscopic and microscopic disease burden in multiple sclerosis based on magnetization transfer.** *AJNR Am J Neuroradiol* 1997;18:1287–1290
19. Poser CM, Paty DW, Scheinberg L, et al. **New diagnostic criteria for multiple sclerosis: guidelines for research protocols.** *Ann Neurol* 1983;13:227–231
20. Udupa J, Samarasekera S. **Fuzzy connectedness and object definition: theory, algorithms, and applications in image segmentation.** *Graph Models Image Process* 1996;58:246–261
21. Udupa JK, Odhner D, Samaraskera S, et al. **3DVIEWNIX: An open, transportable, multidimensional, multimodality, multiparametric imaging software system.** *SPIE Proc* 1994:2164;58–73
22. Udupa J, Wei L, Samarasekera S, Miki Y, van Buchem M, Grossman R. **Detection and quantification of MS lesions using fuzzy topological principles.** *SPIE Proc* 1996:2710;81–91
23. Udupa J, Wei L, Samarasekera S, Miki Y, van Buchem M, Grossman R. **Multiple sclerosis lesion quantification using fuzzy connectedness principles.** *IEEE Trans Med Imaging* 1998 (in press)
24. Dawson JW. **The histology of multiple sclerosis.** *Trans R Soc Edinburgh* 1916;50:517–740
25. Zimmerman HM, Netsky MG. **The pathology of multiple sclerosis.** *Res Publ Assoc Nerv Ment Dis* 1950;28:271–312
26. Brownell B, Hughes JT. **The distribution of plaques in the cerebrum in multiple sclerosis.** *J Neurol Neurosurg Psychiatry* 1962;25: 315–320
27. Barnard RO, Triggs M. **Corpus callosum in multiple sclerosis.** *J Neurol Neurosurg Psychiatry* 1974;37:1259–1264
28. Quattrini A, Paggi A, Ortenzi A, Di Bella P, Cianci F, Forastieri L. **CT and EEG investigations in 100 patients with multiple sclerosis (MS).** *Ital J Neurol Sci* 1981;2:25–34

29. Moseley I. **Computed tomography and nuclear magnetic resonance imaging of the brain in multiple sclerosis: a review.** *Bull Soc Belge Ophthalmol* 1983;208:63–76
30. Loizou LA, Rolfe EB, Hewazy H. **Cranial computed tomography in the diagnosis of multiple sclerosis.** *J Neurol Neurosurg Psychiatry* 1982;45:905–912
31. Jennekens-Schinkel A, Sanders EA. **Decline of cognition in multiple sclerosis: dissociable deficits.** *J Neurol Neurosurg Psychiatry* 1986;49:1354–1360
32. Cala LA, Mastaglia FL, Black JL. **Computerized tomography of brain and optic nerve in multiple sclerosis: observations in 100 patients, including serial studies in 16.** *J Neurol Sci* 1978;36:411–426
33. Gyldensted C. **Computer tomography of the cerebrum in multiple sclerosis.** *Neuroradiology* 1976;12:33–42
34. Reisner T, Maida E. **Computerized tomography in multiple sclerosis.** *Arch Neurol* 1980;37:475–477
35. Rao SM, Glatt S, Hammeke TA, et al. **Chronic progressive multiple sclerosis: relationship between cerebral ventricular size and neuropsychological impairment.** *Arch Neurol* 1985;42:678–682
36. Hageleit U, Will CH, Seidel D. **Automated measurements of cerebral atrophy in multiple sclerosis.** *Neurosurg Rev* 1987;10:137–140
37. Simon JH, Schiffer RB, Rudick RA, Herndon RM. **Quantitative determination of MS-induced corpus callosum atrophy in vivo using MR imaging.** *AJNR Am J Neuroradiol* 1987;8:599–604
38. Huber SJ, Paulson GW, Chakeres D, et al. **Magnetic resonance imaging and clinical correlations in multiple sclerosis.** *J Neurol Sci* 1988;86:1–12
39. Dietemann JL, Beigelman C, Rumbach L, et al. **Multiple sclerosis and corpus callosum atrophy: relationship of MRI findings to clinical data.** *Neuroradiology* 1988;30:478–480
40. Rao SM, Bernardin L, Leo GJ, Ellington L, Ryan SB, Burg LS. **Cerebral disconnection in multiple sclerosis: relationship to atrophy of the corpus callosum.** *Arch Neurol* 1989;46:918–920
41. Comi G, Filippi M, Martinelli V, et al. **Brain magnetic resonance imaging correlates of cognitive impairment in multiple sclerosis.** *J Neurol Sci* 1993;115:S66–S73
42. Damian MS, Schilling G, Bachmann G, Simon C, Stoppler S, Dorndorf W. **White matter lesions and cognitive deficits: relevance of lesion pattern?** *Acta Neurol Scand* 1994;90:430–436
43. Tsolaki M, Drevelegas A, Karachristianou S, Kapinas K, Divanoglou D, Routsonis K. **Correlation of dementia, neuropsychological and MRI findings in multiple sclerosis.** *Dementia* 1994;5:48–52
44. Losseff NA, Wang L, Lai HM, et al. **Progressive cerebral atrophy in multiple sclerosis: a serial MRI study.** *Brain* 1996;119:2009–2019
45. Mehta RC, Pike GB, Enzmann DR. **Measure of magnetization transfer in multiple sclerosis demyelinating plaques, white matter ischemic lesions, and edema.** *Top Magn Reson Imaging* 1996;8:214–230
46. Lexa FJ, Grossman RI, Rosenquist AC. **MR of wallerian degeneration in the feline visual system: characterization by magnetization transfer rate with histopathologic correlation.** *AJNR Am J Neuroradiol* 1994;15:201–212